Excluded-Volume Effects on the Mean-Square Radius of Gyration and Intrinsic Viscosity of Isotactic Oligo- and Poly(methyl methacrylate)s

Masanao Kamijo, Fumiaki Abe, Yoshiyuki Einaga, and Hiromi Yamakawa*

Department of Polymer Chemistry, Kyoto University, Kyoto 606-01, Japan

Received September 28, 1994; Revised Manuscript Received November 10, 1994®

ABSTRACT: The mean-square radius of gyration and intrinsic viscosity were determined for isotactic poly(methyl methacrylate) (i-PMMA) with the fraction of racemic diads $f_r \simeq 0.01$ in acetone at 25.0 °C and in chloroform at 25.0 °C in the range of weight-average molecular weight M_w from 6.58×10^2 to 1.93×10^6. The results for the gyration- and viscosity-radius expansion factors α_S and α_η for i-PMMA along with those previously obtained for atactic poly(methyl methacrylate) (a-PMMA) with $f_r = 0.79$ in the same solvents are found to become functions only of the scaled excluded-volume parameter $\tilde{z}$ defined in the Yamakawa−Stockmayer−Shimada theory on the basis of the helical wormlike chain. Here, α_η for i-PMMA has been calculated as before by taking account of the dependence on solvent of the Flory−Fox factor Φ_0 in the unperturbed state. Thus the present results along with the previous ones for atactic polystyrene (a-PS), polyisobutylene, and a-PMMA lead to the conclusion that the quasi-two-parameter scheme is valid for α_S and α_η for a variety of polymer−solvent systems irrespective of the differences in chain stiffness, local chain conformation, and solvent condition. This also indicates that there is no draining effect on α_η at least for these systems. It is found that the effects of chain stiffness on α_S and α_η remain appreciable even for $M_w > 10^6$ for i-PMMA as well as for a-PS and a-PMMA. The effects are smaller for i-PMMA than for a-PMMA both in acetone and in chloroform, reflecting the fact that the former chain is less stiff than the latter. It is also found that the values of the binary-cluster integral β between beads (segments) for the two PMMAs in the same solvent are almost identical with each other, indicating that β is independent of the stereochemical structure of the polymer chain.

Introduction

In this series of experimental work on the excluded-volume effects in dilute solutions of oligomers and polymers,[1−4] we have shown that a quasi-two-parameter scheme is valid for the gyration- and viscosity-radius expansion factors α_S and α_η for atactic polystyrene (a-PS) with the fraction of racemic diads $f_r = 0.59$, polyisobutylene (PIB), and atactic poly(methyl methacrylate) (a-PMMA) with $f_r = 0.79$. That is, both α_S and α_η for them may be expressed as functions only of the scaled excluded-volume parameter $\tilde{z}$ defined in the Yamakawa−Stockmayer−Shimada (YSS) theory[5−7] that takes account of the effects of excluded-volume and chain stiffness on the basis of the helical wormlike (HW) chain,[8,9] irrespective of the differences in chain stiffness, local chain conformation, and solvent condition. In other words, α_S and α_η are not universal functions of the conventional excluded-volume parameter z, but their changes with z depend on polymer (chain stiffness) and solvent (excluded-volume strength B). It has also been demonstrated that the effects of chain stiffness on α_S and α_η remain large even for such large molecular weight M that the ratio of the unperturbed mean-square radius of gyration $\langle S^2\rangle_0$ to M already reaches its asymptotic coil-limiting value independent of M.

In the present work, we make a similar study of α_S and α_η for isotactic oligo- and poly(methyl methacrylate)s (i-PMMA) with $f_r \simeq 0.01$. From the previous studies of the mean-square radius of gyration $\langle S^2\rangle_\Theta$,[10] intrinsic viscosity $[\eta]_\Theta$,[11] and translational diffusion coefficient D_Θ[11] in the Θ state, it is already known that there are remarkable differences in chain stiffness and local chain conformation between i-PMMA and a-PMMA, which arise from the difference in the stereochemical composition. Thus the main purposes of this paper are 2-fold: (1) confirmation of the validity of the quasi-two-parameter scheme for α_S and α_η for i-PMMA and (2) examination of the differences in the effects of chain stiffness on α_S and α_η and in the excluded-volume strength between the two PMMAs. For these purposes, we determine α_S and α_η of i-PMMA in the same good solvents, i.e., acetone and chloroform at 25.0 °C, as previously used for a-PMMA. As in the previous studies of the excluded-volume effects, we have given particular attention to the correct determination of α_S and α_η, choosing properly a pair of good and Θ solvents so that the values of $\langle S^2\rangle_0$ and $[\eta]_0$ in the unperturbed state in that good solvent may coincide with those of $\langle S^2\rangle_\Theta$ and $[\eta]_\Theta$ in the Θ state taken as the reference standards. In this work, we have confirmed that the values of $\langle S^2\rangle_0$ of i-PMMA in acetone at 25.0 °C agree with those of $\langle S^2\rangle_\Theta$ in acetonitrile at 28.0 °C (Θ) in the oligomer region, where the excluded-volume effect may be negligible.

Experimental Section

Materials. Most of the i-PMMA samples used in this work are the same as those used in the previous studies of $\langle S^2\rangle_\Theta$,[10] $[\eta]_\Theta$,[11] and D_Θ,[11] i.e., the fractions separated by preparative gel permeation chromatography or fractional precipitation from the original samples prepared by living anionic polymerization or from the commercial sample 9011-14-7 from Scientific Polymer Products, Inc. In this work, however, some additional samples with high M were also prepared by fractional precipitation from the latter using acetone as a solvent and hexane as a precipitant. The synthesized samples have a *tert*-butyl group at the initiating chain end and a hydrogen atom at the other end. All the samples have a fixed stereochemical composition ($f_r \simeq 0.01$) independent of M.

The values of the weight-average molecular weight M_w, the weight-average degree of polymerization x_w, and the ratio of M_w to the number-average molecular weight M_n are listed in

® Abstract published in *Advance ACS Abstracts,* January 15, 1995.

0024-9297/95/2228-1095$09.00/0

Table 1. Values of M_w, x_w, and M_w/M_n for Isotactic Oligo- and Poly(methyl methacrylate)s

sample	M_w	x_w	M_w/M_n
iOM6[a]	6.58×10^2	6	1.00
iOM10[a]	1.01×10^3	9.52	1.02
iOM18[a]	1.79×10^3	17.3	1.10
iOM31[a]	3.12×10^3	30.6	1.07
iOM71[b]	7.07×10^3	70.1	1.05
iMM1[a]	1.07×10^4	106	1.05
iMM2[a]	2.57×10^4	256	1.07
iMM3[a]	3.06×10^4	305	1.06
iMMc4[b]	3.68×10^4	367	1.09
iMMc6[b]	5.89×10^4	588	1.08
iMMc9[b]	8.75×10^4	874	1.04
iMMc16[b]	1.55×10^5	1550	1.08
iMMc30[a]	3.13×10^5	3130	1.08
iMMc40	3.80×10^5	3800	1.06
iMMc70	6.88×10^5	6880	1.06
iMMc90[a]	9.46×10^5	9460	1.09
iMMc170[a]	1.71×10^6	17100	1.09
iMMc190	1.93×10^6	19300	1.09

[a] The results have been reproduced from ref 10. [b] The results have been reproduced from ref 11.

Table 1. The samples iMMc40, iMMc70, and iMMc190 are the additional ones and their M_ws were determined from light-scattering (LS) measurements in acetonitrile at 28.0 °C (Θ). The values of M_w/M_n indicate that the molecular weight distributions of all the samples are sufficiently narrow for the present purpose.

The solvents acetonitrile, acetone, and chloroform used for LS, small-angle X-ray scattering (SAXS), and viscosity measurements were purified according to standard procedures.

Light Scattering. LS measurements were carried out to determine $\langle S^2 \rangle$ (and also M_w) of the samples with $M_w \geq 3.16 \times 10^5$ in acetone at 25.0 °C and in chloroform at 25.0 °C and of the three samples iMMc40, iMMc70, and iMMc190 in acetonitrile at 28.0 °C (Θ). A Fica 50 light-scattering photometer was used for all the measurements with vertically polarized incident light of wavelength 436 nm. For a calibration of the apparatus, the intensity of light scattered from pure benzene was measured at 25.0 °C at a scattering angle of 90°, where the Rayleigh ratio $R_{Uu}(90°)$ of pure benzene was taken as 46.5×10^{-6} cm^{-1}. The depolarization ratio ϱ_u of pure benzene at 25.0 °C was found to be 0.41 ± 0.01. Scattering intensities were measured at seven or eight different concentrations and at scattering angles ranging from 30° to 142.5° except for iMMc190 in acetone and iMMc70, iMMc90, and iMMc190 in chloroform. For these, the intensities were measured at 10–12 scattering angles ranging from 15° to 120°. All the data obtained were analyzed by the Berry square-root plot.[12]

The most concentrated solutions of each sample were prepared by continuous stirring at room temperature or at 50 °C for ca. 1 day in the two good solvents, especially preventing the chloroform solution from being exposed to light, and at ca. 50 °C for 2 days in acetonitrile. They were optically purified by filtration through a Teflon membrane of pore size 0.45 or 0.10 μm. The solutions of lower concentrations were obtained by successive dilution. The polymer mass concentrations c were calculated from the weight fractions with the densities of the solutions. The densities of the solvents and solutions were measured with a pycnometer of the Lipkin–Davison type.

The value of the refractive index increment $\partial n/\partial c$ measured with a Shimadzu differential refractometer at 436 nm was 0.065_0 cm^3/g for i-PMMA with $M_w \gtrsim 3.0 \times 10^4$ in chloroform at 25.0 °C. For the values of $\partial n/\partial c$ at 436 nm for i-PMMA in the other solvents, the results previously[10] reported were used.

Small-Angle X-ray Scattering. SAXS measurements were carried out for the i-PMMA samples with $M_w \lesssim 3.0 \times 10^4$ in acetone at 25.0 °C and for the oligomer sample iOM71 in acetonitrile at 28.0 °C (Θ) by the use of an Anton Paar Kratky U-slit camera with an incident X-ray of wavelength 1.54 Å (Cu Kα line). The apparatus system and the method of data acquisition and analysis are the same as those described in the previous paper.[13]

The measurements were performed for five or six solutions of different concentrations for each polymer sample and for the solvent at scattering angles ranging from 1×10^{-3} rad to a value at which the scattering intensity was negligibly small. Corrections for the stability of the X-ray source and the detector electronics were made by measuring the intensity scattered from Lupolene (a platelet of polyethylene) used as a working standard before and after each measurement of a given sample solution and the solvent. The effect of absorption of X-ray by a given solution or solvent was also corrected by measuring the intensity scattered from Lupolene with insertion of the solution or solvent between the X-ray source and Lupolene. The degree of absorption increased linearly with increasing solute concentration.

The excess reduced scattering intensity $\Delta I_R(k)$ as a function of the magnitude k of the scattering vector was determined from the observed (smeared) excess reduced intensities by the modified Glatter desmearing method, which consists of expressing the true scattering function in terms of cubic B-spline functions, as previously[13] described, where k is given by

$$k = (4\pi/\lambda_0) \sin(\theta/2) \tag{1}$$

with λ_0 the wavelength of the incident X-ray and θ the scattering angle. All the data were processed by the use of a Fujitsu M-1800/30 digital computer in this university. Then the data for $\Delta I_R(k)$ were analyzed by the Berry square-root plot as in the case of LS data to determine the apparent mean-square radius of gyration $\langle S^2 \rangle_s$. The $\langle S^2 \rangle$ of the chain contour was then obtained from $\langle S^2 \rangle_s$ as before by the use of the equation

$$\langle S^2 \rangle_s = \langle S^2 \rangle + S_c^2 \tag{2}$$

which was derived for a continuous chain having a uniform circular cross section with S_c being the radius of gyration of the cross section.[13] In this work, we make the above correction by adopting the value 8.2 Å^2 of S_c^2 estimated from the data for the partial specific volume v_2 of i-PMMA in acetonitrile at 28.0 °C, as done previously.[10] We note that the value of v_2 of i-PMMA in acetone at 25.0 °C is approximately equal to that in acetonitrile at 28.0 °C for sufficiently large M_w.

The test solutions of each sample were prepared in the same manner as in the case of LS measurements.

Viscosity. Viscosity measurements were carried out for almost all the samples in acetone at 25.0 °C and in chloroform at 25.0 °C, and also for the three samples iMMc40, iMMc70, and iMMc190 in acetonitrile at 28.0 °C (Θ). We used four-bulb spiral capillary viscometers of the Ubbelohde type. Viscosities of the chloroform solutions of the sample iMMc190 were measured at very low shear rate so that the non-Newtonian effect might be ignored. In all the measurements, the flow time was measured to a precision of 0.1 s, keeping the difference between those of the solvent and solution larger than ca. 20 s. The test solutions were maintained at constant temperature within ±0.005 °C during the measurements. The data obtained were treated as usual by the Huggins and Fuoss–Mead plots to determine $[\eta]$ and the Huggins coefficient k'.

The test solutions were prepared in the same manner as in the case of LS measurements. Density corrections were made in the calculations of c and also of the relative viscosity from the flow times of the solution and solvent.

Results

Mean-Square Radius of Gyration. The values of the root-mean-square radius of gyration $\langle S^2 \rangle^{1/2}$ obtained for i-PMMA in acetone at 25.0 °C and in chloroform at 25.0 °C from SAXS and LS measurements are listed in Table 2 along with those of M_w determined from LS measurements. (Those values of M_w of the same sample in the different solvents agree with each other within experimental error.) Figure 1 shows double-logarithmic plots of the ratio $(\langle S^2 \rangle/x_w)/(\langle S^2 \rangle_\Theta/x_w)_{\infty,a}$ against x_w with

Table 2. Results of SAXS and LS Measurements on Isotactic Oligo- and Poly(methyl methacrylate)s in Acetone at 25.0 °C and in Chloroform at 25.0 °C

	acetone, 25.0 °C		chloroform, 25.0 °C	
sample	$10^{-4}M_w$	$\langle S^2\rangle^{1/2}$, Å	$10^{-4}M_w$	$\langle S^2\rangle^{1/2}$, Å
iOM6		5.27		
iOM10		7.64		
iOM31		16.0		
iOM71		25.1		
iMM1		31.4		
iMM3		55.6		
iMMc30	31.6	203	31.6	264
iMMc40	37.9	226	38.5	296
iMMc70	68.6	314	69.4	421
iMMc90	97.8	383	97.8	515
iMMc190	197	574	197	778

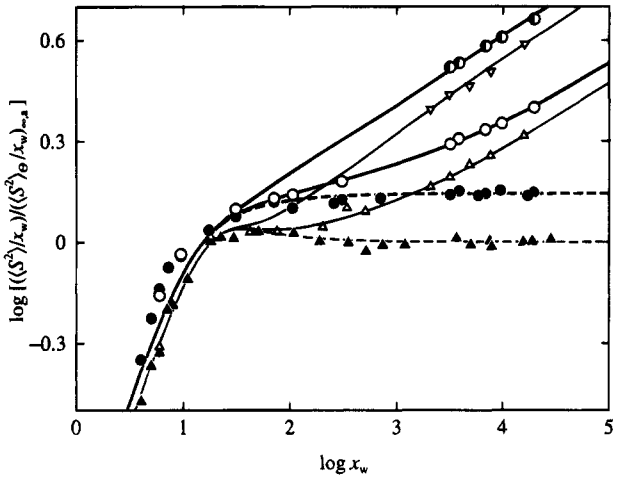

Figure 1. Double-logarithmic plots of $(\langle S^2\rangle/x_w)/(\langle S^2\rangle_\Theta/x_w)_{\infty,a}$ against x_w for the i-PMMA samples with $f_r \simeq 0.01$ and for the a-PMMA samples with $f_r = 0.79$, where $(\langle S^2\rangle_\Theta/x_w)_{\infty,a}$ denotes the asymptotic value of $\langle S^2\rangle/x_w$ for a-PMMA in acetonitrile at Θ: (○) i-PMMA in acetone at 25.0 °C; (◐) i-PMMA in chloroform at 25.0 °C; (●) i-PMMA in acetonitrile at 28.0 °C (Θ) (reproduced from ref 10, except for the samples iOM71, iMMc40, iMMc70, and iMMc190); (△) a-PMMA in acetone at 25.0 °C; (▽) a-PMMA in chloroform at 25.0 °C; (▲) a-PMMA in acetonitrile at 44.0 °C (Θ). The data for a-PMMA have been reproduced from refs 4 and 14. The solid and dashed curves represent the best-fit YSS and HW theory values for the perturbed and unperturbed chains, respectively (see text).

Table 3. Results of SAXS, LS, and Viscosity Measurements on Isotactic Oligo- and Poly(methyl methacrylate)s in Acetonitrile at 28.0 °C (Θ)

sample	$10^{-4}M_w$	$\langle S^2\rangle_\Theta^{1/2}$, Å	$[\eta]_\Theta$, dL/g	k'
iOM71		24.8		
iMMc40	38.0	190	0.590	0.64
iMMc70	68.8	253	0.794	0.61
iMMc190	193	425	1.35	0.71

the present data for i-PMMA in acetone at 25.0 °C (unfilled circles) and in chloroform at 25.0 °C (half-filled circles) along with those previously[10] obtained in acetonitrile at 28.0 °C (Θ) (filled circles), where, for convenience, $\langle S^2\rangle/x_w$ has been divided by the asymptotic value $(\langle S^2\rangle_\Theta/x_w)_{\infty,a}$ of $\langle S^2\rangle_\Theta/x_w$ in the limit of $x_w \to \infty$ for a-PMMA (not for i-PMMA) in acetonitrile at 44.0 °C (Θ), which has been taken as 6.57 Å^2.[4,14] (For the acetonitrile solutions, $\langle S^2\rangle$ refers to $\langle S^2\rangle_\Theta$.) The figure includes the data obtained in this work for the samples iOM71, iMMc40, iMMc70, and iMMc190 in acetonitrile at Θ, which are given in Table 3 along with those for $[\eta]_\Theta$. For comparison, it also includes the results previously obtained for a-PMMA in the same good and Θ solvents (unfilled and filled triangles).[4,14] For convenience, we have not drawn the solid and dashed curves which connect the data points smoothly but those which represent the best-fit YSS and HW theory values calculated for the perturbed and unperturbed chains, respectively, with the values of the HW model parameters and the excluded-volume strength B previously[4,10,14] determined, as described in the Discussion section, where the values of B for i-PMMA in the two good solvents have been determined. (The values of the HW model parameters and B are listed later in Table 5.) (We note that the values of the exponent in the power law relating $\langle S^2\rangle^{1/2}$ to M_w estimated from the data for $M_w > 10^5$ are 0.58_3 and 0.56_2 in chloroform at 25.0 °C and in acetone at 25.0 °C, respectively.)

It is seen that the values of $\langle S^2\rangle$ in acetone at 25.0 °C agree with those in acetonitrile at Θ in the oligomer region for $M_w \lesssim 3 \times 10^3$. This agreement implies that $\langle S^2\rangle_0$ of the i-PMMA chain in acetone at 25.0 °C may be considered to be identical with its $\langle S^2\rangle_\Theta$ in acetonitrile at Θ, so that we may calculate correctly α_S for i-PMMA at least in acetone by the use of the values of $\langle S^2\rangle_\Theta$ in acetonitrile as the reference standards. The critical value ca. 30 of x_w for the onset of the excluded-volume effect in the i-PMMA chain in acetone corresponds to the value ca. 2.4 of the reduced contour length, which is close to the corresponding value ca. 1.9 for a-PMMA in the same solvent. For both PMMAs in acetone, $\langle S^2\rangle/x_w$ increases with increasing x_w for $x_w \gtrsim 10^2$, following curves that convex downward. However, the curvature of the curve for i-PMMA is smaller than that for a-PMMA. This difference may be regarded as arising from the differences in chain stiffness and local chain conformation between the two PMMAs, which has been discussed in the preceding paper.[10]

Now, recall that the values of $\langle S^2\rangle_\Theta$ for a-PMMA (with large M_w) in the two Θ solvents, acetonitrile at 44.0 °C and *n*-butyl chloride at 40.8 °C, coincide with each other[14,15] and that the values of $\langle S^2\rangle$ for its oligomers in acetone at 25.0 °C coincide with those of $\langle S^2\rangle_\Theta$ in the former Θ solvent.[4] Thus it has been concluded that the dependence of its $\langle S^2\rangle_0$ on solvent is negligibly small, and then its α_S in all the good solvents examined has been calculated by taking the values of $\langle S^2\rangle_\Theta$ in acetonitrile at Θ as the reference standards. In the present work, we also calculate α_S for i-PMMA in chloroform as well as in acetone at 25.0 °C by the use of the values of $\langle S^2\rangle_\Theta$ in acetonitrile at Θ, although the dependence of $\langle S^2\rangle_0$ or $\langle S^2\rangle_\Theta$ on solvent for i-PMMA has not been examined extensively. (We tried to determine the Θ temperature and evaluate $\langle S^2\rangle_\Theta$ for i-PMMA in *n*-butyl chloride, but the attempt was unsuccessful because of the incomplete solubility of i-PMMA in that solvent.)

Intrinsic Viscosity. The values of $[\eta]$ determined for all the samples in acetone at 25.0 °C and in chloroform at 25.0 °C are summarized in Table 4 along with those of k'. Figure 2 shows double-logarithmic plots of $[\eta]/M_w^{1/2}$ ($[\eta]$ in dL/g) against M_w with the data in acetone (unfilled circles) and those in chloroform (half-filled circles) along with those previously[11] obtained in acetonitrile at 28.0 °C (Θ) (filled circles). The figure includes the data obtained in this work for the samples iMMc40, iMMc70, and iMMc190 in acetonitrile at Θ, which are given in Table 3 along with those for k'. For comparison, it also includes the results previously obtained for a-PMMA in the same good and Θ solvents (unfilled and filled triangles).[4,15] The solid and dashed curves connect the data points smoothly. (We note that the values of the Houwink–Mark–Sakurada

Table 4. Results of Viscometry on Isotactic Oligo- and Poly(methyl methacrylate)s in Acetone at 25.0 °C and in Chloroform at 25.0 °C

	acetone, 25.0 °C		chloroform, 25.0 °C	
sample	$[\eta]$, dL/g	k'	$[\eta]$, dL/g	k'
iOM10	0.0300	0.89		
iOM18			0.0455	0.71
iOM31	0.0533	0.74		
iOM71	0.0831	0.66		
iMM1	0.100	0.63	0.133	0.45
iMM2	0.161	0.54	0.236	0.38
iMM3	0.188	0.52		
iMMc4	0.203	0.61		
iMMc6	0.276	0.50	0.460	0.37
iMMc9	0.343	0.67		
iMMc16	0.492	0.49	0.931	0.35
iMMc30	0.782	0.49	1.60	0.32
iMMc40	0.885	0.43	1.85	0.35
iMMc70	1.33	0.51	2.85	0.35
iMMc90	1.66	0.42	3.80	0.34
iMMc170	2.39	0.52		
iMMc190	2.66	0.43	6.43	0.33

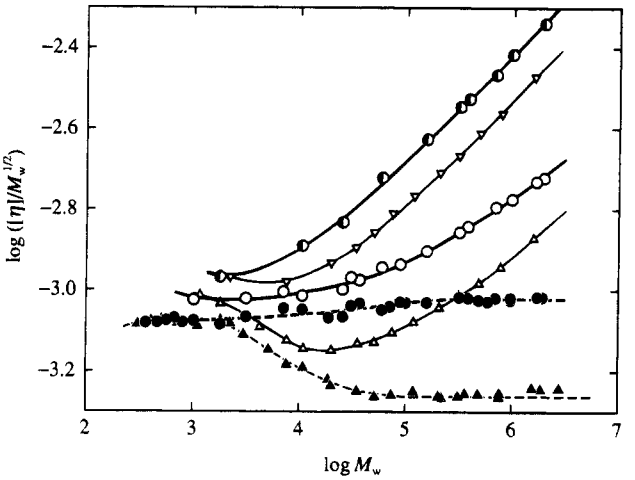

Figure 2. Double-logarithmic plots of $[\eta]/M_w^{1/2}$ ($[\eta]$ in dL/g) against M_w for i-PMMA and a-PMMA. The symbols have the same meaning as those in Figure 1. The data for i-PMMA in acetonitrile at Θ have been reproduced from ref 11 except for the samples iMMc40, iMMc70, and iMMc190, and those for a-PMMA, from refs 4 and 15. The solid and dashed curves connect the data points smoothly.

exponent estimated from the data for $M_w > 10^5$ are 0.76_9 and 0.66_4 in chloroform at 25.0 °C and in acetone at 25.0 °C, respectively.)

For i-PMMA in acetone, $[\eta]/M_w^{1/2}$ increases monotonically with increasing M_w except in the oligomer region, while for a-PMMA in acetone it first decreases, then passes through a minimum, and finally increases with increasing M_w. This difference may also be regarded as arising from the differences in chain stiffness and local chain conformation between the two PMMAs as in the case of $\langle S^2\rangle/x_w$ above.

In the oligomer region for $M_w \lesssim 2 \times 10^3$, the values of $[\eta]/M_w^{1/2}$ for the two PMMAs coincide with each other in either good solvent as well as in acetonitrile at Θ. This may be due to the fact that the average chain dimension in that region and also the hydrodynamic bead diameter (in the HW touched-bead model) are almost independent of f_r. However, the values of $[\eta]$ in acetone are definitely larger than those in acetonitrile at Θ even in the oligomer region, despite the fact that the values of $\langle S^2\rangle$ there in the two solvents agree with each other, as shown in Figure 1. The value of $[\eta]$ of the oligomer sample iOM18 in chloroform is also significantly larger than that in acetonitrile at Θ. These results imply that the bead diameter depends appreciably on solvent. Thus the Flory–Fox factor Φ_Θ may possibly depend on solvent as in the case of a-PMMA.[15,16] Necessarily, this leads to the introduction of the apparent viscosity-radius expansion factor $\bar{\alpha}_\eta$ for i-PMMA as well as for a-PMMA.[4]

Discussion

Gyration-Radius Expansion Factor α_S. We first analyze the present data for α_S^2 on the basis of the YSS theory[5-7] for the perturbed HW chain. It may be calculated from

$$\langle S^2\rangle = \langle S^2\rangle_0 \alpha_S^2 \tag{3}$$

with the values of $\langle S^2\rangle^{1/2}$ given in Table 2 and those of $\langle S^2\rangle_\Theta^{1/2}$ previously[10] determined and also given in Table 3, assuming that $\langle S^2\rangle_\Theta^{1/2} = \langle S^2\rangle_0^{1/2}$, as mentioned above.

Now it is convenient to reproduce necessary basic equations. For the HW chain of total contour length L, the theory assumes the Domb–Barrett expression[17] for α_S^2, i.e.,

$$\alpha_S^2 = [1 + 10\tilde{z} + (70\pi/9 + 10/3)\tilde{z}^2 + 8\pi^{3/2}\tilde{z}^3]^{2/15} \times [0.933 + 0.067\ \exp(-0.85\tilde{z} - 1.39\tilde{z}^2)] \tag{4}$$

with the scaled excluded-volume parameter $\tilde{z}$ defined by

$$\tilde{z} = (^3/_4)K(\lambda L)z \tag{5}$$

in place of the conventional excluded-volume parameter z. The latter is now defined by

$$z = (3/2\pi)^{3/2}(\lambda B)(\lambda L)^{1/2} \tag{6}$$

where

$$B = \beta/a^2 c_\infty^{3/2} \tag{7}$$

with

$$c_\infty = \lim_{\lambda L\to\infty} (6\lambda\langle S^2\rangle_0/L) = \frac{4 + (\lambda^{-1}\tau_0)^2}{4 + (\lambda^{-1}\kappa_0)^2 + (\lambda^{-1}\tau_0)^2} \tag{8}$$

Here, λ^{-1} is the static stiffness parameter of the HW chain, κ_0 and τ_0 are the differential-geometrical curvature and torsion, respectively, of its characteristic helix taken at the minimum zero of its elastic energy, β is the binary-cluster integral between beads with a their spacing (in the touched-bead model). In eq 5, the coefficient $K(L)$ is given by

$$K(L) = {}^4/_3 - 2.711L^{-1/2} + {}^7/_6 L^{-1} \quad \text{for } L > 6$$
$$= L^{-1/2}\exp(-6.611L^{-1} + 0.9198 + 0.03516L) \quad \text{for } L \le 6 \tag{9}$$

Note that L is related to the degree of polymerization x by the equation

$$L = xM_0/M_L \tag{10}$$

where M_0 is the molecular weight of the repeat unit of

Table 5. Values of the HW Model Parameters, the Reduced Excluded-Volume Strength λB, and the Binary-Cluster Integral β for Isotactic and Atactic Poly(methyl methacrylate)s

polymer (f_r)	solvent	temp, °C	$\lambda^{-1}\kappa_0$	$\lambda^{-1}\tau_0$	λ^{-1}, Å	M_L, Å^{-1}	λB	β, Å^3
i-PMMA (0.01)	acetonitrile[a]	28.0	2.5	1.3	38.0	32.5	0	0
	acetone	25.0	(2.5)	(1.3)	(38.0)	(32.5)	0.10	12
	chloroform	25.0	(2.5)	(1.3)	(38.0)	(32.5)	0.55	65
a-PMMA (0.79)	acetonitrile[b]	44.0	4.0	1.1	57.9	36.3	0	0
	acetone[c]	25.0	(4.0)	(1.1)	(57.9)	(36.3)	0.22	12
	chloroform[c]	25.0	(4.0)	(1.1)	(57.9)	(36.3)	1.15	62

[a] See ref 10. [b] See ref 14. [c] See ref 4.

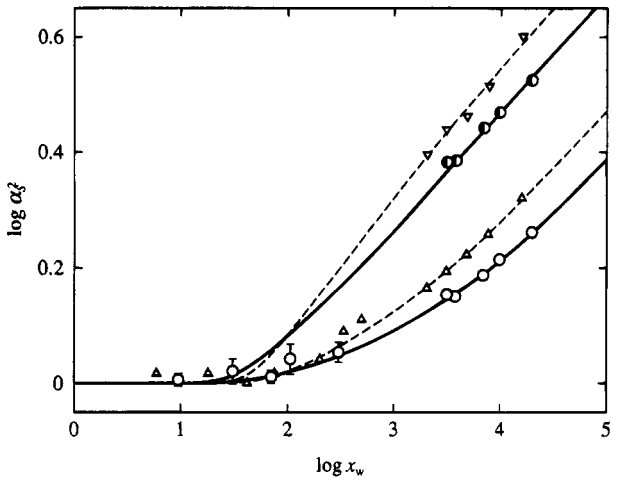

Figure 3. Double-logarithmic plots of α_S^2 against x_w for i-PMMA and a-PMMA in acetone at 25.0 °C and in chloroform at 25.0 °C. The symbols have the same meaning as those in Figure 1. The vertical line segments indicate the limit of experimental error. The solid and dashed curves represent the best-fit YSS theory values (see text).

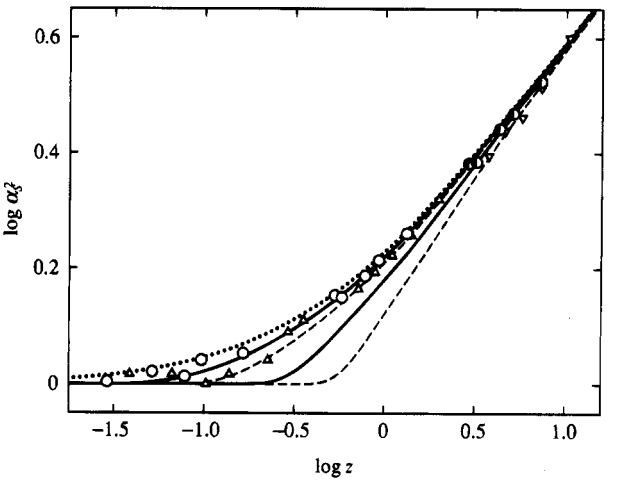

Figure 4. Double-logarithmic plots of α_S^2 against z for i-PMMA and a-PMMA in acetone at 25.0 °C and in chloroform at 25.0 °C. The symbols have the same meaning as those in Figure 1. The solid and dashed curves represent the best-fit YSS theory values, and the dotted curve represents the conventional two-parameter-theory values (see text).

a given real chain and M_L is the shift factor as defined as the molecular weight per unit contour length.

In order to analyze the experimental values of α_S, we need the values of the HW model parameters $\lambda^{-1}\kappa_0$, $\lambda^{-1}\tau_0$, λ^{-1}, and M_L, and the reduced excluded-volume strength λB. The values of the HW model parameters for i-PMMA[10] already determined from a comparison of the experimental values of $\langle S^2 \rangle_\Theta$ in acetonitrile at Θ with the HW theory have been reproduced in the first row of Table 5. The corresponding results previously obtained for a-PMMA[14] have also been reproduced in the fourth row, for comparison. We may adopt those parameter values for i-PMMA in the good solvents used in this study, provided that $\langle S^2 \rangle_0 = \langle S^2 \rangle_\Theta$ as is always the case. The remaining parameter λB may be determined from a comparison of the experimental values of α_S with the YSS theory, as done previously.[1-4]

Figure 3 shows double-logarithmic plots of α_S^2 against x_w for i-PMMA in the two good solvents, acetone (unfilled circles) and chloroform (half-filled circles). It also includes the previous results for a-PMMA in the same solvents (unfilled triangles),[4] for comparison. The vertical line segments attached to the unfilled circles indicate the limit of experimental error for SAXS measurements. The solid curves represent the best-fit YSS theory values calculated from eq 4 with eqs 5, 6, 9, and 10. (The dashed curves also represent the best-fit YSS theory values previously calculated for a-PMMA in the same manner.) The values of λB thus determined from the curve fitting are given in the eighth column of Table 5, where the previous results for a-PMMA are also given. It is seen that the theoretical critical value of x_w for the onset of the excluded-volume effect in the i-PMMA chain is almost independent of solvent as in the case of a-PMMA. This value for i-PMMA is somewhat smaller than that for a-PMMA, but the corresponding values of the reduced contour length λL for them are close to each other (as mentioned above for the acetone solutions). Note that at fixed x_w for $x_w \lesssim 10^2$, the value of α_S^2 for i-PMMA is larger than that for a-PMMA.

The values of λB for i-PMMA in acetone and in chloroform are seen to be remarkably smaller than the corresponding values for a-PMMA. However, it is very interesting to see from the last column of Table 5 that the values of β itself calculated from eq 7 for the two PMMAs by taking the repeat unit as a single bead (with $a = M_0/M_L$) are very close to each other both in acetone and in chloroform. This indicates that the excluded-volume interaction (β) between beads is independent of the stereochemical structure of the polymer chain, so that the difference in α_S between the two PMMAs in the same solvent, as shown in Figure 3, arises from the differences in chain stiffness and local chain conformation between them.

The same data for α_S^2 as in Figure 3 are double-logarithmically plotted against z in Figure 4, where the values of z have been calculated from eq 6 with eq 10 and with the values of the parameters given in Table 5. The solid and dashed curves represent the YSS theory values for i-PMMA and a-PMMA, respectively. For comparison, the two-parameter-theory values calculated from eq 4 with $\tilde{z} = z$ are represented by the dotted curve. The data points for i-PMMA and the solid curves fitted to them do not form a single composite curve but deviate progressively downward from the dotted curve with decreasing z (or decreasing L) because of the effect of chain stiffness as in the case of a-PMMA.

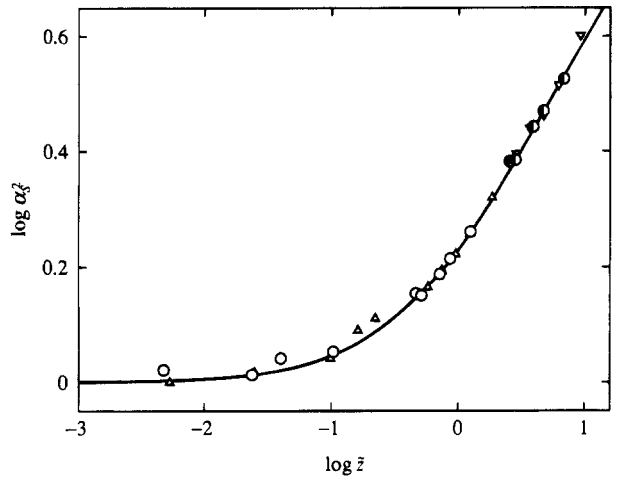

Figure 5. Double-logarithmic plots of α_S^2 against $\tilde{z}$ for i-PMMA and a-PMMA in acetone at 25.0 °C and in chloroform at 25.0 °C. The symbols have the same meaning as those in Figure 1. The solid curve represents the YSS theory values (see text).

The deviation becomes more significant as λB is increased or, in other words, as the solvent quality becomes better. The effect of chain stiffness on α_S remains rather large even for large $z > 10$ or $M_w > 10^6$ for i-PMMA as well as for a-PMMA and also a-PS.[1]

Figure 5 shows double-logarithmic plots of α_S^2 against $\tilde{z}$ with the same data as in Figures 3 and 4, where the values of $\tilde{z}$ have been calculated from eq 5 with eq 9 and with the above values of z, and the solid curve represents the YSS theory values calculated from eq 4. It is seen that the data points for the two PMMAs in the two different solvents form a single composite curve and that there is good agreement between theory and experiment over the whole range of $\tilde{z}$ or M_w studied. This result confirms the previous conclusion[1-4] that the quasi-two-parameter scheme for α_S is valid irrespective of the large differences in chain stiffness, local chain conformation, and solvent quality.

Viscosity-Radius Expansion Factor α_η^3. As mentioned above, the present data for $[\eta]$ suggest that the Flory–Fox factor Φ_Θ depends on solvent for i-PMMA as well as for a-PMMA.[15,16] Thus they must be analyzed in the new scheme previously[4] presented. It is then convenient to begin by summarizing necessary basic equations.

The intrinsic viscosity $[\eta]$ in a given good solvent may be written as usual in the form

$$[\eta] = 6^{3/2}\Phi\frac{\langle S^2\rangle_0^{3/2}}{M}\alpha_S^3 \tag{11}$$

This is rather the defining equation for the Flory–Fox factor Φ (in that good solvent). We then define the cubed true and apparent viscosity-radius expansion factors α_η^3 and $\bar{\alpha}_\eta^3$ by the equations

$$[\eta] = [\eta]_0\alpha_\eta^3 = [\eta]_\Theta\bar{\alpha}_\eta^3 \tag{12}$$

with

$$[\eta]_0 = 6^{3/2}\Phi_0\frac{\langle S^2\rangle_0^{3/2}}{M} \tag{13}$$

and

$$[\eta]_\Theta = 6^{3/2}\Phi_\Theta\frac{\langle S^2\rangle_\Theta^{3/2}}{M} \tag{14}$$

where $[\eta]_0$ and Φ_0 denote the values of $[\eta]$ and Φ in the unperturbed state in the good solvent, respectively, and $[\eta]_\Theta$ and Φ_Θ denote those of $[\eta]$ and Φ in a given Θ solvent at Θ, respectively. (Note that the coil-limiting value $\Phi_{\Theta,\infty}$ of Φ_Θ is in general not a universal constant but depends not only on solvent but also on polymer, as previously shown.[11,16]) Thus, even if the relation $\langle S^2\rangle_0 = \langle S^2\rangle_\Theta$ holds, Φ_0 is not always equal to Φ_Θ. Then, if $\langle S^2\rangle_0 = \langle S^2\rangle_\Theta$, we have, from eqs 11 − 14

$$\bar{\alpha}_\eta^3 = C_\eta\alpha_\eta^3 = C_\eta\alpha_\Phi\alpha_S^3 \tag{15}$$

where C_η and α_Φ are defined by

$$C_\eta = \Phi_0/\Phi_\Theta \tag{16}$$

and

$$\alpha_\Phi = \Phi/\Phi_0 \tag{17}$$

If the quasi-two-parameter scheme is valid, both α_η and α_Φ must be functions only of $\tilde{z}$, and the $\bar{\alpha}_\eta^3$ must be of the form

$$\bar{\alpha}_\eta^3 = C_\eta f(\alpha_S) \tag{18}$$

where f is a function only of α_S. Note that the coefficient C_η is essentially identical with the constant prefactor that has been previously[15] introduced to represent the dependence of $\Phi_{\Theta,\infty}$ for a-PMMA on solvent.

We have calculated the values of $\bar{\alpha}_\eta^3$ for i-PMMA in the two good solvents from the second equality of eq 12 with the values of $[\eta]$ given in Table 3 and those of $[\eta]_\Theta$ obtained in the present and previous work,[11] limiting the calculation to the range of $M_w \geq 7.07 \times 10^3$ because of the possible effect of the dependence of the bead diameter on solvent. The values of $\bar{\alpha}_\eta^3$ obtained are double-logarithmically plotted against α_S^3 in Figure 6 (unfilled and half-filled circles), where the previous results for a-PMMA in the same solvents (triangles)[4] are also included, for comparison. The solid curve is the one that connects smoothly the data points for a-PS in various solvents previously reported.[2-4] It is seen that the data points for i-PMMA in each solvent deviate upward from the solid curve by a certain constant independent of α_S^3, as shown by the dashed curve. The results are qualitatively the same as those for a-PMMA, although the deviation is smaller for i-PMMA than for a-PMMA in either solvent.

Now, according to eq 15, the above constant deviation of the data points for i-PMMA in each solvent in Figure 6 may be equated to log C_η as in the case of a-PMMA, since we may put $C_\eta = 1$ for a-PS.[4] Recall that $\Phi_{\Theta,\infty}$ of a-PS is independent of solvent (as far as cyclohexane and *trans*-decalin are concerned).[16] The values of C_η thus estimated from the separations between the solid and heavy dashed curves are 1.04 and 1.12 for i-PMMA in acetone and in chloroform, respectively, which are smaller than the corresponding values for a-PMMA.

With these values of C_η, we have calculated α_η^3 from the first equality of eq 15 with the values of $\bar{\alpha}_\eta^3$ determined above. The results are double-logarithmically plotted against z in Figure 7 (unfilled and half-filled circles), where we have calculated again the values of z from eq 6 with eq 10 with the values of the

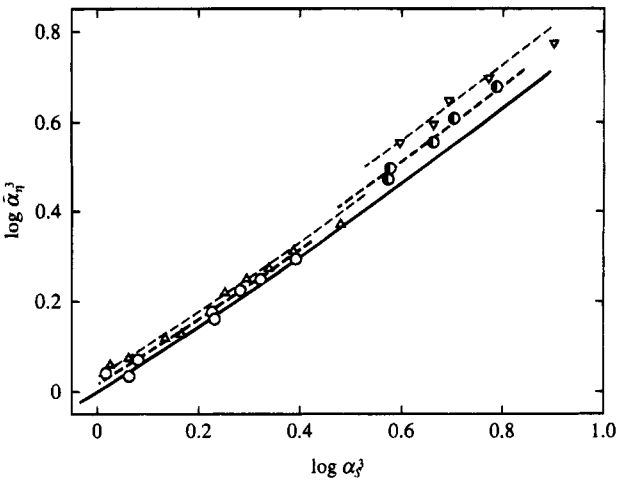

Figure 6. Double-logarithmic plots of $\bar{\alpha}_\eta^3$ against α_S^3 for i-PMMA and a-PMMA in acetone at 25.0 °C and in chloroform at 25.0 °C. The symbols have the same meaning as those in Figure 1. The solid curve represents the best-fit one for the experimental data for a-PS in various solvents. The dashed curves connect the data points smoothly for i-PMMA and a-PMMA (see text).

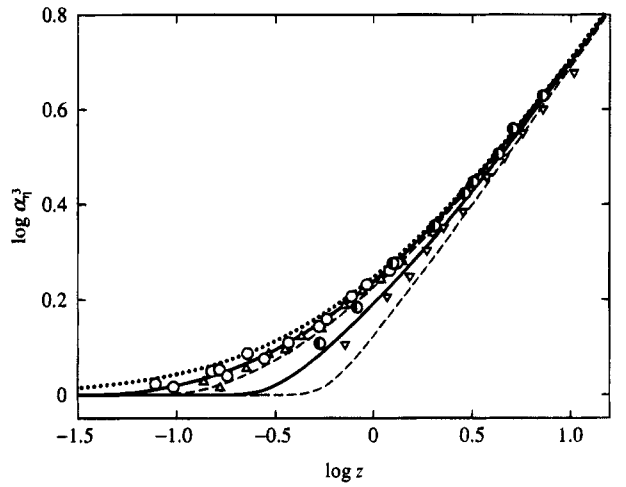

Figure 7. Double-logarithmic plots of α_η^3 against z for i-PMMA and a-PMMA in acetone at 25.0 °C and in chloroform at 25.0 °C. The symbols have the same meaning as those in Figure 1. The solid and dashed curves represent the theoretical values calculated from eq 19 with the values of the HW model parameters and λB given in Table 5 and the dotted curve represents the two-parameter-theory values (see text).

parameters given in Table 5. The solid curves represent the theoretical values calculated from the Barrett equation[18] for α_η with $\tilde{z}$ in place of z, i.e.,

$$\alpha_\eta^3 = (1 + 3.8\tilde{z} + 1.9\tilde{z}^2)^{0.3} \qquad (19)$$

with eqs 5, 6, 9, and 10 and with the values of the parameters given in Table 5. The dotted curve represents the two-parameter-theory values calculated from eq 19 with $\tilde{z} = z$. Figure 7 also includes the previous results for a-PMMA in the same solvents (unfilled triangles and dashed curves),[4] for comparison.

The solid curves are seen to agree rather well with the data points over the whole range of z studied, although there is some disagreement in chloroform. It is also seen that the data points (or the solid curves) deviate progressively downward from the dotted curve with decreasing z (or M_w), the deviation being more significant for larger λB (excluded-volume strength), because of the effect of chain stiffness. The effect

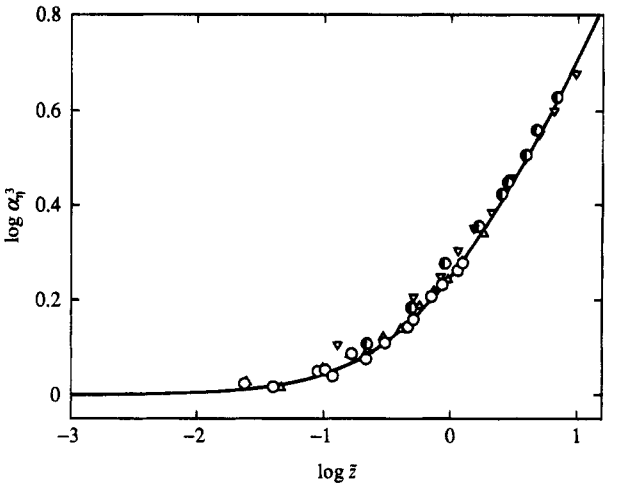

Figure 8. Double-logarithmic plots of α_η^3 against $\tilde{z}$ for i-PMMA and a-PMMA in acetone at 25.0 °C and in chloroform at 25.0 °C. The symbols have the same meaning as those in Figure 1. The solid curve represents the theoretical values calculated from eq 19.

remains appreciable even for large $z > 10$ or $M_w > 10^6$ as in the cases of a-PMMA and a-PS.[2,3] However, it is less remarkable for i-PMMA than for a-PMMA in either solvent, reflecting the fact that the i-PMMA chain is less stiff than the a-PMMA chain.[10,11] All these features for α_η as a function of z are quite similar to those for α_S shown in Figure 4.

Figure 8 shows double-logarithmic plots of α_η^3 against $\tilde{z}$ with the same data for i-PMMA (unfilled and half-filled circles) and a-PMMA (unfilled triangles) as in Figure 7, where the values of $\tilde{z}$ have been calculated again from eq 5 with eq 9 and with the above values of z. The solid curve represents the theoretical values calculated from eq 19. The data points for i-PMMA in acetone and in chloroform form a single-composite curve together with those for a-PMMA in the same solvents. It has already been shown that the latter data also form a single-composite curve together with those for a-PS in various solvents and for PIB in n-heptane.[4] Thus it may be concluded that α_η is a function only of $\tilde{z}$, or in other words, the quasi-two-parameter scheme is valid for α_η as well as for α_S, irrespective of the difference in f_r or the differences in chain stiffness and local chain conformation. The present results also indicate that there is no draining effect on α_η for i-PMMA as well as for the other systems stated above. Finally, we must claim that the solid curve does not (no longer) seem to reproduce completely the experimental results over the whole range of $\tilde{z}$ studied, the former curvature being somewhat larger than the latter. (The equivalent disagreement between theory and experiment is already recognized in Figure 7.)

Conclusion

We have made a study of α_S and α_η as functions of z and $\tilde{z}$ for i-PMMA with $f_r \simeq 0.01$ in acetone at 25.0 °C and in chloroform at 25.0 °C and compared the results with those previously[4] obtained for a-PMMA with $f_r = 0.79$ in the same solvents. The values of α_η for i-PMMA in the two good solvents have been calculated by taking account of the dependence of Φ_Θ or Φ_0 on solvent as in the case of a-PMMA, i.e., by dividing the cubed apparent viscosity-radius expansion factor $\bar{\alpha}_\eta^3$ determined in the conventional way by the constant factor C_η that explains the dependence of Φ_0 on solvent. It is then found that both α_S and α_η become functions only of $\tilde{z}$ for i-PMMA

as well as for a-PS,[1-3] PIB,[2] and a-PMMA.[4] Thus it may be concluded that the quasi-two-parameter scheme is valid for α_S and α_η for a variety of polymer–solvent systems irrespective of the large differences in chain stiffness, local chain conformation, and solvent condition. The results for α_η indicate that there is no draining effect on α_η for i-PMMA as well as for the other polymers. It is also concluded that the experimental $\alpha_S(\tilde{z})$ may be quantitatively explained by the YSS theory with the use of the Domb–Barrett equation[17] for α_S, while the experimental $\alpha_\eta(\tilde{z})$ cannot be completely explained by the corresponding theory with the Barrett equation[18] for α_η.

Both α_S and α_η as functions of z deviate progressively downward from the two-parameter-theory prediction with decreasing z or M_w, the deviation being more significant for larger λB (excluded-volume strength), because of the effects of chain stiffness, as previously found for a-PS and a-PMMA.[1-4] These effects on α_S and α_η remain rather large even for large $z > 10$ or $M_w > 10^6$ for i-PMMA as well as for the other polymers. However, it is found that the effects are smaller for i-PMMA than for a-PMMA in the same solvent, since the i-PMMA chain is less stiff than the a-PMMA chain.

When compared at fixed x_w (except for $x_w \lesssim 10^2$), the value of α_S for i-PMMA is smaller than that for a-PMMA both in acetone and in chloroform. The results lead to a smaller value of λB for i-PMMA than for a-PMMA in either solvent. However, there is good agreement between the values of β itself for the two PMMAs in the same solvent. This indicates that the excluded-volume interaction between beads is independent of the stereochemical structure of the polymer chain, so that the above difference in α_S between the two PMMAs in the same solvent arises from the differences in chain stiffness and local chain conformation between them.

References and Notes

(1) Abe, F.; Einaga, Y.; Yoshizaki, T.; Yamakawa, H. *Macromolecules* **1993**, *26*, 1884.
(2) Abe, F.; Einaga, Y.; Yamakawa, H. *Macromolecules* **1993**, *26*, 1891.
(3) Horita, K.; Abe, F.; Einaga, Y.; Yamakawa, H. *Macromolecules* **1993**, *26*, 5067.
(4) Abe, F.; Horita, K.; Einaga, Y.; Yamakawa, H. *Macromolecules* **1994**, *27*, 725.
(5) Yamakawa, H.; Stockmayer, W. H. *J. Chem. Phys.* **1972**, *57*, 2843.
(6) Yamakawa, H.; Shimada, J. *J. Chem. Phys.* **1985**, *83*, 2607.
(7) Shimada, J.; Yamakawa, H. *J. Chem. Phys.* **1986**, *85*, 591.
(8) Yamakawa, H. *Annu. Rev. Phys. Chem.* **1984**, *35*, 23.
(9) Yamakawa, H. In *Molecular Conformation and Dynamics of Macromolecules in Condensed Systems*; Nagasawa, M., Ed.; Elsevier: Amsterdam, 1988; p 21.
(10) Kamijo, M.; Sawatari, N.; Konishi, T.; Yoshizaki, T.; Yamakawa, H. *Macromolecules* **1994**, *27*, 5697.
(11) Sawatari, N.; Konishi, T.; Yoshizaki, T.; Yamakawa, H. *Macromolecules* **1995**, *28*, xxxx (preceding paper in this issue).
(12) Berry, G. C. *J. Chem. Phys.* **1966**, *44*, 4550.
(13) Konishi, T.; Yoshizaki, T.; Saito, T.; Einaga, Y.; Yamakawa, H. *Macromolecules* **1990**, *23*, 290.
(14) Tamai, Y.; Konishi, T.; Einaga, Y.; Fujii, M.; Yamakawa, H. *Macromolecules* **1990**, *23*, 4067.
(15) Fujii, Y.; Tamai, Y.; Konishi, T.; Yamakawa, H. *Macromolecules* **1991**, *24*, 1608.
(16) Konishi, T.; Yoshizaki, T.; Yamakawa, H. *Macromolecules* **1991**, *24*, 5614.
(17) Domb, C.; Barrett, A. J. *Polymer* **1976**, *17*, 179.
(18) Barrett, A. J. *Macromolecules* **1984**, *17*, 1566.

MA941160W